

Radial velocity precision of ESPRESSO through the analysis of the solar twin HIP 11915

YURI NETTO,¹ DIEGO LORENZO-OLIVEIRA,¹ JORGE MELÉNDEZ,¹
JHON YANA GALARZA,¹ RAPHAËLLE D. HAYWOOD,² LORENZO SPINA,³ AND
LEONARDO A. DOS SANTOS⁴

¹*Universidade de São Paulo, Instituto de Astronomia, Geofísica e Ciências Atmosféricas (IAG), Departamento de Astronomia, Rua do Matão 1226, Cidade Universitária, 05508-900, SP, Brazil*

²*Astrophysics Group, University of Exeter, Exeter EX4 4QL, UK*

³*INAF Osservatorio Astronomico di Padova, vicolo dell'Osservatorio 5, 35122, Padova, Italy*

⁴*Observatoire Astronomique de l'Université de Genève, Chemin Pegasi 51, 1290 Versoix, Switzerland*

(Received xxxx; Revised yyyy; Accepted zzzz)

ABSTRACT

Different stellar phenomena affect radial velocities (RVs), causing variations large enough to make it difficult to identify planet signals from the stellar variability. RV variations caused by stellar oscillations and granulation can be reduced through some methods, but the impact of rotationally modulated magnetic activity on RV, due to stellar active regions is harder to correct. New instrumentation promises an improvement in precision of one order of magnitude, from about 1 m/s, to about 10 cm/s. In this context, we report our first results from 24 spectroscopic ESPRESSO/VLT observations of the solar twin star HIP 11915, spread over 60 nights. We used a Gaussian Process approach and found for HIP 11915 a RV residual RMS scatter of about 20 cm s⁻¹, representing an upper limit for the performance of ESPRESSO.

Keywords: techniques: radial velocities - methods: data analysis - stars: individual: HIP 11915

1. INTRODUCTION

The radial velocity (RV) method has been used to discover exoplanets, or to confirm exoplanets detected by the transit method and estimate their mass. Earth analogs orbiting the habitable zone of a Sun-like star, induce a RV signal on the order of 10 cm s⁻¹ (e.g., [Langellier et al. 2020](#)). However, the measured RV variations are not entirely due to planets; stellar activity, oscillations and granulation also cause changes in RV

(e.g., Fischer et al. 2016). The effect of stellar oscillations and granulation on RV can be reduced by adopting exposure times tailored to the star’s spectral type (Chaplin et al. 2019), or modelling through magnetohydrodynamical simulations (Cegla et al. 2016). Yet, the impact of rotationally modulated stellar activity is hard to predict, as stellar activity cycles are not strictly periodic and have complex shapes. Furthermore, the presence of active regions on the stellar surface can induce RV signals, which can sometimes be mis-interpreted as planet signals (e.g. Figueira et al. 2010; Haywood et al. 2014; Díaz et al. 2018).

Thus, a better understanding and characterisation of the impact of stellar activity on RV is crucial for the progress in our ability to detect exoplanets (Blackwood et al. 2020). After the discovery of the first exoplanet around solar-type stars (Mayor & Queloz 1995), Saar & Donahue (1997) discussed the possible impact of apparent changes in RV due to the effects of stellar magnetic activity. Further, Hatzes (2002) and Desort et al. (2007) also presented characterisation of the likely effects of stellar active regions. More recently the interest has been renewed (e.g., Haywood et al. 2020; Bauer et al. 2018; Borgniet et al. 2015; Korhonen et al. 2015; Dumusque et al. 2014), as planet searches are focusing in small exoplanets, for which the stellar activity imposes serious limitations in their detection.

Observations and models show the dependence of the RV-activity on the activity cycle phase (e.g., Borgniet et al. 2015; Korhonen et al. 2015), being the lowest at the activity cycle minimum. There have been important advances in the treatment of star-induced RV variability, through reconstructing the geometry of active regions (e.g, Dumusque et al. 2014) or semi empirically through a Gaussian process (GP) fit (e.g, Haywood et al. 2014). GP regression (Rajpaul et al. 2015; Roberts et al. 2012) has become one of the most successful tools in the analysis of stellar activity in RV time series (Dumusque et al. 2017).

The aim of this work is to test the accuracy of the RV uncertainties estimated by the ESPRESSO data reduction pipeline, reported to be at a precision level of 10 cm s^{-1} (Pepe et al. 2020). For this, we analyse RV observations of the solar twin HP 11915, which is currently in the minimum of its magnetic activity cycle; we account for rotationally modulated stellar activity using GP regression. Details regarding the data are in Section 2. In Section 3 we present the method to analyse the RV. We discuss our results in Section 4.

2. OBSERVATIONS AND DATA REDUCTIONS

The new high-resolution spectrograph ESPRESSO (*Echelle SPectrograph for Rocky Exoplanets and Stable Spectroscopic Observations*, Pepe et al. 2014, 2020) of ESO’s Very-Large Telescope (VLT) started operations at the ESO Paranal observatory in September 2018. It is designed and built to detect and characterise Earth analogs within the habitable zones of their host stars, reaching RV precision of 10 cm s^{-1} . More details regarding ESPRESSO may be found in the general description of the

ESPRESSO instrument, reported on the actual on-sky performance described by [Pepe et al. \(2020\)](#).

The solar twin star HIP 11915 was selected from our former HARPS planet survey around solar twins, from which a Jupiter-twin planet was found ([Bedell et al. 2015](#)). The star has been carefully characterised in our previous works ([Galarza et al. 2021](#); [Spina et al. 2018](#); [dos Santos et al. 2016](#)), with improved Ca II H&K activity indices derived by [Lorenzo-Oliveira et al. \(2018\)](#). In Table 1 we summarise the main fundamental parameters derived for HIP 11915. Within the ESO program 0102.C-0523 (PI: Jorge Meléndez), we obtained a total of 24 observations of HIP 11915 from November 2018 to January 2019. Measurements were taken in ESPRESSO’s High Resolution 1-UT (HR) mode to reach a high resolving power ($R = \lambda/\Delta\lambda = 140\,000$). We reduced the spectra using the 1.3.2¹ version of the ESOReflex environment ([Freudling et al. 2013](#)). The data reduction includes the standard procedures such as corrections for bias, flat-field and background light, wavelength calibration, extraction of the spectrum, merging of the Echelle orders, and barycentric and instrumental drift corrections. The resulting spectra are given in counts and calibrated in flux. The wavelength calibration is performed combining a Thorium-Argon (Th-Ar) hollow-cathode lamp and a white-light illuminated Fabry-Pérot. The former provides wavelength accuracy, and the latter ensures wavelength precision. The pipeline also provides a cross-correlation function (CCF), computed with respect to a binary template mask. Then, the RV is obtained from a Gaussian fit to the CCF. For each exposure, we extracted the RV and activity indicators from the CCF (Full width at half maximum, FWHM, and CCF CONTRAST). The activity index S is measured from the extracted spectra, following prescriptions given in [Wright et al. \(2004\)](#). The contrast of the CCF, expressed as a percentage, is the relative depth of the CCF at its central wavelength, used to measure temporal changes ([Lafarga et al. 2020](#)). [Maldonado et al. \(2019\)](#) found significant correlations between the contrast with the main optical activity indicators for the Sun-as-a-star observations.

3. RV PERFORMANCE THROUGH GP ANALYSIS

The star-induced RV variability is difficult to model deterministically, and has motivated the use of GP regression ([Haywood et al. 2014](#); [Rajpaul et al. 2015](#)). GP is a powerful statistical technique, in which intrinsic stellar variability is treated as correlated noise described by a covariance functional form, while the hyper-parameters describe the physical phenomena to be modelled. A kernel function is chosen to model these covariances as a function between two measurements at a time ([Haywood et al. 2014](#); [Rajpaul et al. 2015](#); [Faria et al. 2016](#)).

3.1. *Gaussian Process Model*

¹ <https://www.eso.org/sci/software/esoreflex/>

Table 1. Fundamental parameters for HIP 11915.

Parameter	Value	Reference
Spectral Type	G5V	[1]
V(mag)	8.615	[2]
T_{eff} (K)	5773 ± 2	[3]
[Fe/H]	-0.057 ± 0.003	[3]
$\log g$	4.470 ± 0.008	[3]
$\log R'_{\text{HK}}(T_{\text{eff}})$	-4.923 ± 0.028	[4]
Age (Gyr)	3.87 ± 0.39	[3]
Mass (M_{\odot})	0.991 ± 0.003	[3]
$P_{\text{rot}}/\sin(i)$ (d)	42.0 ± 8.6	[5]
Number of observations	24	

NOTE—[1] Houk & Smith-Moore (1988), [2] Ramírez et al. (2012), [3] Galarza et al. (2021), [4] Lorenzo-Oliveira et al. (2018), [5] Lorenzo-Oliveira et al. (2019)

For a given activity indicator i , we define a combination of covariance functions between two measurements at time t and t' of the observations, to build our quasi-periodic (QP) activity model:

$$k(t, t') \equiv \mathcal{I}_{\text{const}} + \mathcal{A} \exp \left(-\frac{\|t - t'\|}{2\ell^2} - \Gamma \sin^2 \left[\frac{\pi}{P_{\text{rot}}} \|t - t'\| \right] \right) + \sigma^2 \delta_{t,t'}, \quad (1)$$

where $\mathcal{I}_{\text{const}}$ gives a constant scale to match the observed mean activity level of the star, while \mathcal{A} represents the amplitude of the rotation signal. The timescale of rising and decay of active regions is interpreted by ℓ , the harmonic nature of the time series is represented by Γ , the white noise term is $\sigma^2 \delta_{t,t'}$ and P_{rot} is the rotational period, where P_{rot} was initially determined by using generalised Lomb-Scargle periodograms (GLS, Zechmeister & Kürster 2009). We use a log-normal prior distribution for the hyper-parameters (HP): $\mathcal{I}_{\text{const}}$ ($\mu = \langle i \rangle$, $\sigma = \sigma_{\langle i \rangle}$), P_{rot} ($\mu = P_{\text{rot}}$, $\sigma = 0.2 \times P_{\text{rot, GLS}}$), and $\ln \Gamma$ ($\mu = -2.3$, $\sigma = 1.4$, as in Angus et al. 2018). We use the *emcee* (Foreman-Mackey et al. 2013) Python implementation of the affine-invariant Markov chain Monte Carlo method (MCMC) following Angus et al. (2018) to estimate the posterior distribution of all GP HP. In brief, we start the MCMC process with 64 walkers to sample the parameter space, and are initialised with an optimal solution obtained by maximum likelihood optimisation. Then, every 100 steps, we evaluate the convergence of chains and check its auto-correlation timescale (τ_{chain}) and the consistency of walkers solutions through Gelman-Rubin statistics (\hat{R}) (Gelman & Rubin 1992). We consider that the walkers have converged when τ_{chain} is less than 10 % of the total chain length, τ_{chain} is stable concerning the previous chain evaluation within 1%, and \hat{R} less than 1.03. Finally, we discard the initial iterations ($3 \times \tau_{\text{chain}}$) and

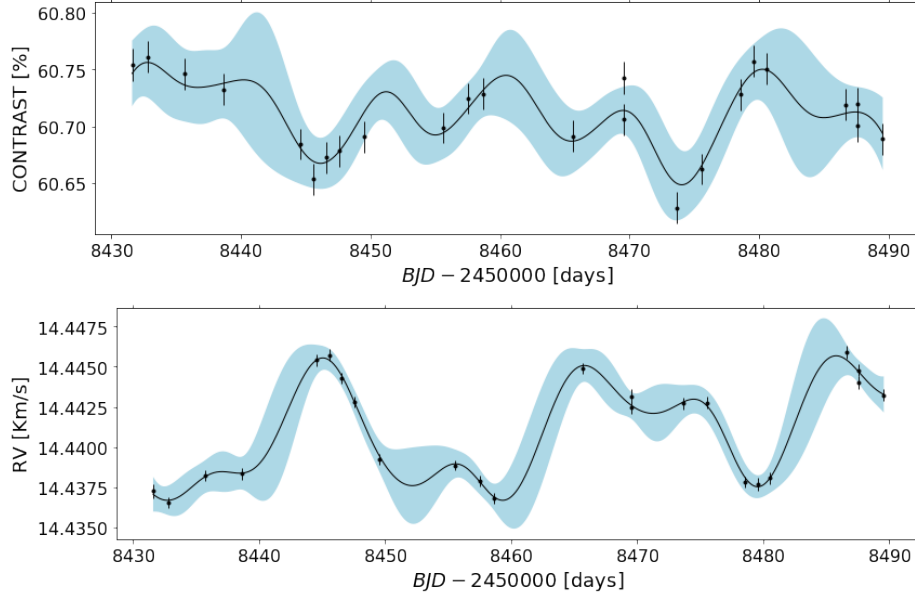


Figure 1. GP regression fits to ~ 60 days of CONTRAST (upper panel) and RV data (lower panel) of HIP 11915, both from ESPRESSO. Solid lines and shaded blue regions are the QP model and 2σ predictions, respectively.

randomly re-sample 5000 samples to represent our estimate of posterior probability distribution of all GP hyper-parameters.

3.2. Fitting the RV

To model the RV of HIP 11915 we fit the activity indicator i and the RV consecutively. We fit the RV using the same QP kernel function of equation 1 with the Γ , P_{cycle} and ℓ fixed at the median value from the activity indicator i fit. The GP regression fit to the CONTRAST and to the RV are shown in Fig. 1. The resulting HP estimates are displayed in the last column of Table 2 as the median and 16 % confidence interval of these uncorrelated samples. We also applied the same procedure to the FWHM and the S Index and its resulting HP estimates for the RV are displayed in the bottom part of the Table 2.

The root mean square (RMS) of the residuals is 25 cm s^{-1} , 23 cm s^{-1} and 23 cm s^{-1} for the RMS $\text{res}_{\text{CONTRAST,RV}}$, RMS $\text{res}_{\text{FWHM,RV}}$ and RMS $\text{res}_{\text{SIndex,RV}}$, respectively. These values can be compared to the average RV uncertainty of 27 cm s^{-1} . They are also in agreement with the posterior estimate for the white noise term parameters of 20 cm s^{-1} , yet at the level of few tens of cm s^{-1} . In Fig. 2, we show all the residuals for each fit. The values reached for the RV precision are robust, since the GP was applied independently for each activity indicator.

To test the stability of the values found for the total sample, we re-sampled 30 times, choosing the observations randomly, keeping 2/3 of the total sample. The results remained relatively stable, deviating $+6 \text{ cm s}^{-1}$ from the original values, except for the FWHM which had the largest deviation, 11 cm s^{-1} . The HP also remained stable in tests, most of them resulting in the same value found for the total sample. The

Table 2. Summary of hyper-parameters, upper and lower bounds of the priors and its initial guesses used for Markov chain Monte Carlo (MCMC) sampling for the CONTRAST (CONT) and RV fits of ESPRESSO data. The last column shows the resulting median value of the MCMC samples and their corresponding error.

	Fit HP	MCMC initial guess	Priors Bounds	Fit Value
CONT HP	$\mathcal{I}_{\text{CONT}}$ [%]	mean(CONT)	(60.628, 60.761)	60.710 $^{+0.021}_{-0.023}$
	σ_{CONT} [%]	mean(CONT error)	(0.0022, 0.0226)	0.0134 $^{+0.0043}_{-0.0033}$
	$\mathcal{A}_{\text{CONT}}$ [%]	var(CONT)	(0.034, 0.174)	0.059 $^{+0.030}_{-0.016}$
	ℓ [d]	30	(2, 365)	68.8 $^{+68.1}_{-27.6}$
	Γ	0.1	(-10, 2)	2.5 $^{+1.9}_{-1.3}$
	P_{rot} [d]	24.03 (GLS)	(15, 50)	27.4 $^{+1.2}_{-7.9}$
RV HP	$\mathcal{I}_{\text{CONT,RV}}$ [km s $^{-1}$]	mean(RV)	(14.436, 14.446)	14.441 \pm 0.002
	$\sigma_{\text{CONT,RV}}$ [km s $^{-1}$]	mean(RV error)	(10 $^{-4}$, 5 \times 10 $^{-3}$)	0.0002 \pm 0.0001
	$\mathcal{A}_{\text{CONT,RV}}$ [km s $^{-1}$]	var(RV)	(0.0032, 0.0160)	0.0039 $^{+0.0008}_{-0.0037}$
RV HP	$\mathcal{I}_{\text{FWHM,RV}}$ [km s $^{-1}$]	mean(RV)	(14.436, 14.446)	14.441 \pm 0.002
	$\sigma_{\text{FWHM,RV}}$ [km s $^{-1}$]	mean(RV error)	(10 $^{-4}$, 5 \times 10 $^{-3}$)	0.0002 \pm 0.0001
	$\mathcal{A}_{\text{FWHM,RV}}$ [km s $^{-1}$]	var(RV)	(0.0032, 0.0160)	0.0037 $^{+0.0006}_{-0.0003}$
RV HP	$\mathcal{I}_{\text{SIndex,RV}}$ [km s $^{-1}$]	mean(RV)	(14.436, 14.446)	14.441 \pm 0.001
	$\sigma_{\text{SIndex,RV}}$ [km s $^{-1}$]	mean(RV error)	(10 $^{-4}$, 5 \times 10 $^{-3}$)	0.0002 \pm 0.0001
	$\mathcal{A}_{\text{SIndex,RV}}$ [km s $^{-1}$]	var(RV)	(0.0032, 0.0160)	0.0037 $^{+0.0005}_{-0.0003}$

HP ℓ and Γ present greater variation in results, from \sim 60 days to \sim 200 days and \sim 0.5 to \sim 2.5, respectively.

We also used the GP approach applied to the recently released ESO Phase 3 (pipeline version 2.2.1 or higher), to test if different pipelines to reduce the data interfere with the results. The results remained relatively stable, the root mean square (RMS) of the residuals is 24 cm s $^{-1}$, 41 cm s $^{-1}$ and 44 cm s $^{-1}$ for the RMS $\text{res}_{\text{CONTRAST,RV}}$, RMS $\text{res}_{\text{FWHM,RV}}$ and RMS $\text{res}_{\text{SIndex,RV}}$, respectively.

4. CONCLUSIONS

In this work we report results about the ESPRESSO RV precision. Using the solar twin HIP 11915 data (\sim 60 days) from the ESPRESSO spectrograph at the VLT, we applied the Gaussian Process regression with a quasi-periodic kernel to obtain the residuals from the fits. We found an average value of 24 cm s $^{-1}$ for the RMS of our residuals, that represents an upper limit for the performance of ESPRESSO for this range of observation. HIP 11915 is a solar twin star, observed during the minimum of its activity cycle, and the low activity level of the star has helped to evaluate the performance of ESPRESSO, demonstrating that the instrument can achieve low-to-mid 20 cm/s on quiet stars.

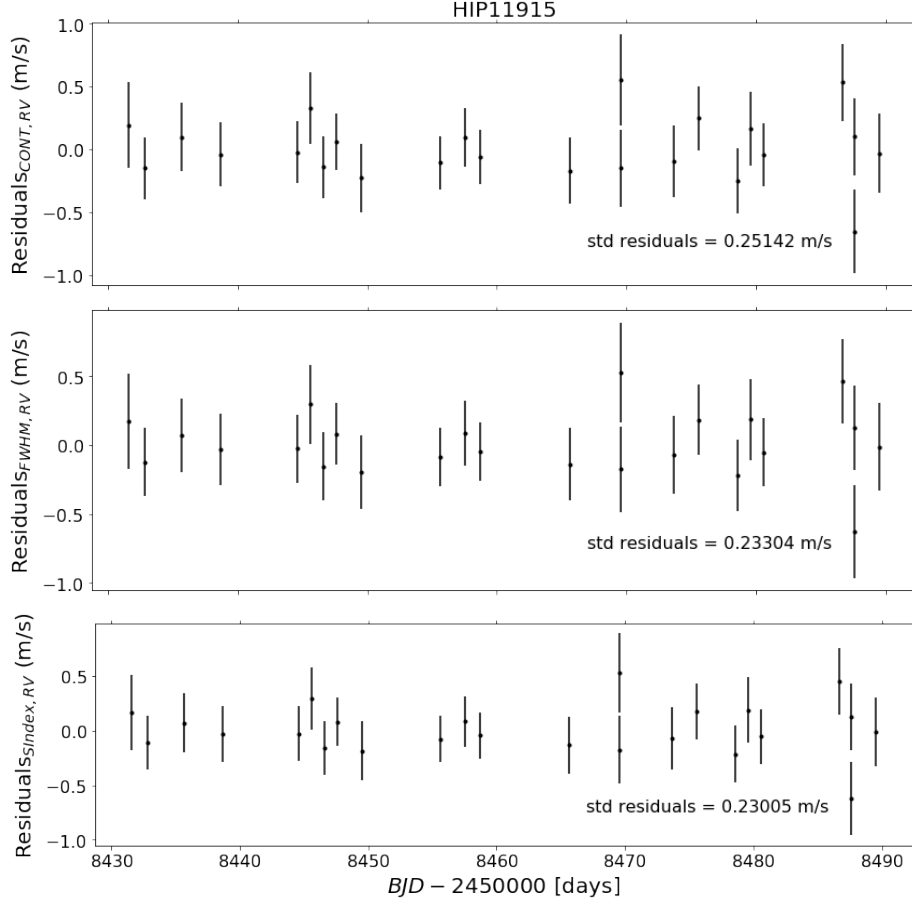


Figure 2. Residuals in radial velocities of the GP fit for each activity indicator with its rms scatter. In each panel, the GP was trained on: **Top:** CONTRAST; **Middle:** FWHM; **Bottom:** S Index.

With long-term repeated measurements, it may be possible to improve the RV precision for the HIP 11915. This is a great target for the searches of Earth analogs, since it has a Jupiter twin (Bedell et al. 2015), has a chemical composition depleted in rocky-forming elements, similar to the Sun (Galarza et al. 2021), and a precision at the level of 20 cm s^{-1} can be achieved.

ACKNOWLEDGMENTS

Y.N. and J.M. thanks support from FAPESP (2019/20319-8; 2018/04055-8). D.L.O. and J.M. thanks support from FAPESP (2016/20667-8; 2018/04055-8). J.Y.G. acknowledges the support from CNPq (142084/2017-4). LAdS acknowledges the support of NCCR PlanetS, the Swiss National Science Foundation, and the European Research Council under programme No 724427 (project FOUR ACES).

Facility: **ESO:** VLT 8.2-meter Unit Telescopes, Echelle SPectrograph for Rocky Exoplanet and Stable Spectroscopic Observations (ESPRESSO).

REFERENCES

- Angus, R., Morton, T., Aigrain, S., Foreman-Mackey, D., & Rajpaul, V. 2018, *MNRAS*, 474, 2094, doi: [10.1093/mnras/stx2109](https://doi.org/10.1093/mnras/stx2109)
- Bauer, F. F., Reiners, A., Beeck, B., & Jeffers, S. V. 2018, *A&A*, 610, A52, doi: [10.1051/0004-6361/201731227](https://doi.org/10.1051/0004-6361/201731227)
- Bedell, M., Meléndez, J., Bean, J. L., et al. 2015, *A&A*, 581, A34, doi: [10.1051/0004-6361/201525748](https://doi.org/10.1051/0004-6361/201525748)
- Blackwood, G., Gaudi, B. S., Burt, J., et al. 2020, in *American Astronomical Society Meeting Abstracts*, Vol. 235, American Astronomical Society Meeting Abstracts #235, 374.01
- Borgniet, S., Meunier, N., & Lagrange, A. M. 2015, *A&A*, 581, A133, doi: [10.1051/0004-6361/201425007](https://doi.org/10.1051/0004-6361/201425007)
- Cegla, H. M., Oshagh, M., Watson, C. A., et al. 2016, *ApJ*, 819, 67, doi: [10.3847/0004-637X/819/1/67](https://doi.org/10.3847/0004-637X/819/1/67)
- Chaplin, W. J., Cegla, H. M., Watson, C. A., Davies, G. R., & Ball, W. H. 2019, *AJ*, 157, 163, doi: [10.3847/1538-3881/ab0c01](https://doi.org/10.3847/1538-3881/ab0c01)
- Desort, M., Lagrange, A. M., Galland, F., Udry, S., & Mayor, M. 2007, *A&A*, 473, 983, doi: [10.1051/0004-6361:20078144](https://doi.org/10.1051/0004-6361:20078144)
- Díaz, M. R., Jenkins, J. S., Tuomi, M., et al. 2018, *AJ*, 155, 126, doi: [10.3847/1538-3881/aaa896](https://doi.org/10.3847/1538-3881/aaa896)
- dos Santos, L. A., Meléndez, J., do Nascimento, J.-D., et al. 2016, *A&A*, 592, A156, doi: [10.1051/0004-6361/201628558](https://doi.org/10.1051/0004-6361/201628558)
- Dumusque, X., Boisse, I., & Santos, N. C. 2014, *ApJ*, 796, 132, doi: [10.1088/0004-637X/796/2/132](https://doi.org/10.1088/0004-637X/796/2/132)
- Dumusque, X., Borsa, F., Damasso, M., et al. 2017, *A&A*, 598, A133, doi: [10.1051/0004-6361/201628671](https://doi.org/10.1051/0004-6361/201628671)
- Faria, J. P., Haywood, R. D., Brewer, B. J., et al. 2016, *A&A*, 588, A31, doi: [10.1051/0004-6361/201527899](https://doi.org/10.1051/0004-6361/201527899)
- Figueira, P., Marmier, M., Bonfils, X., et al. 2010, *A&A*, 513, L8, doi: [10.1051/0004-6361/201014323](https://doi.org/10.1051/0004-6361/201014323)
- Fischer, D. A., Anglada-Escude, G., Arriagada, P., et al. 2016, *PASP*, 128, 066001, doi: [10.1088/1538-3873/128/964/066001](https://doi.org/10.1088/1538-3873/128/964/066001)
- Foreman-Mackey, D., Hogg, D. W., Lang, D., & Goodman, J. 2013, *PASP*, 125, 306, doi: [10.1086/670067](https://doi.org/10.1086/670067)
- Freudling, W., Romaniello, M., Bramich, D. M., et al. 2013, *A&A*, 559, A96, doi: [10.1051/0004-6361/201322494](https://doi.org/10.1051/0004-6361/201322494)
- Galarza, J. Y., Meléndez, J., Karakas, A. I., Asplund, M., & Lorenzo-Oliveira, D. 2021, *MNRAS*, doi: [10.1093/mnras/rlab010](https://doi.org/10.1093/mnras/rlab010)
- Gelman, A., & Rubin, D. B. 1992, *Statistical Science*, 7, 457, doi: [10.1214/ss/1177011136](https://doi.org/10.1214/ss/1177011136)
- Hatzes, A. P. 2002, *Astronomische Nachrichten*, 323, 392, doi: [10.1002/1521-3994\(200208\)323:3/4<392::AID-ASNA392>3.0.CO;2-M](https://doi.org/10.1002/1521-3994(200208)323:3/4<392::AID-ASNA392>3.0.CO;2-M)
- Haywood, R. D., Collier Cameron, A., Queloz, D., et al. 2014, *MNRAS*, 443, 2517, doi: [10.1093/mnras/stu1320](https://doi.org/10.1093/mnras/stu1320)
- Haywood, R. D., Milbourne, T. W., Saar, S. H., et al. 2020, *arXiv e-prints*, arXiv:2005.13386, <https://arxiv.org/abs/2005.13386>
- Houk, N., & Smith-Moore, M. 1988, *Michigan Catalogue of Two-dimensional Spectral Types for the HD Stars. Volume 4, Declinations -26°.0 to -12°.0.*, Vol. 4
- Korhonen, H., Andersen, J. M., Piskunov, N., et al. 2015, *MNRAS*, 448, 3038, doi: [10.1093/mnras/stu2730](https://doi.org/10.1093/mnras/stu2730)
- Lafarga, M., Ribas, I., Lovis, C., et al. 2020, *A&A*, 636, A36, doi: [10.1051/0004-6361/201937222](https://doi.org/10.1051/0004-6361/201937222)

- Langellier, N., Milbourne, T. W., Phillips, D. F., et al. 2020, arXiv e-prints, arXiv:2008.05970.
<https://arxiv.org/abs/2008.05970>
- Lorenzo-Oliveira, D., Freitas, F. C., Meléndez, J., et al. 2018, *A&A*, 619, A73, doi: [10.1051/0004-6361/201629294](https://doi.org/10.1051/0004-6361/201629294)
- Lorenzo-Oliveira, D., Meléndez, J., Yana Galarza, J., et al. 2019, *MNRAS*, 485, L68, doi: [10.1093/mnrasl/slz034](https://doi.org/10.1093/mnrasl/slz034)
- Maldonado, J., Phillips, D. F., Dumusque, X., et al. 2019, *A&A*, 627, A118, doi: [10.1051/0004-6361/201935233](https://doi.org/10.1051/0004-6361/201935233)
- Mayor, M., & Queloz, D. 1995, *Nature*, 378, 355, doi: [10.1038/378355a0](https://doi.org/10.1038/378355a0)
- Pepe, F., Molaro, P., Cristiani, S., et al. 2014, *Astronomische Nachrichten*, 335, 8, doi: [12.1002/asna.201312004](https://doi.org/10.1002/asna.201312004)
- Pepe, F., Cristiani, S., Rebolo, R., et al. 2020, arXiv e-prints, arXiv:2010.00316.
<https://arxiv.org/abs/2010.00316>
- Rajpaul, V., Aigrain, S., Osborne, M. A., Reece, S., & Roberts, S. 2015, *MNRAS*, 452, 2269, doi: [10.1093/mnras/stv1428](https://doi.org/10.1093/mnras/stv1428)
- Ramírez, I., Michel, R., Sefako, R., et al. 2012, *ApJ*, 752, 5, doi: [10.1088/0004-637X/752/1/5](https://doi.org/10.1088/0004-637X/752/1/5)
- Roberts, S., Osborne, M., Ebdem, M., et al. 2012, *Philosophical Transactions of the Royal Society of London Series A*, 371, 20110550, doi: [10.1098/rsta.2011.0550](https://doi.org/10.1098/rsta.2011.0550)
- Saar, S. H., & Donahue, R. A. 1997, *ApJ*, 485, 319, doi: [10.1086/304392](https://doi.org/10.1086/304392)
- Spina, L., Meléndez, J., Karakas, A. I., et al. 2018, *MNRAS*, 474, 2580, doi: [10.1093/mnras/stx2938](https://doi.org/10.1093/mnras/stx2938)
- Wright, J. T., Marcy, G. W., Butler, R. P., & Vogt, S. S. 2004, *ApJS*, 152, 261, doi: [10.1086/386283](https://doi.org/10.1086/386283)
- Zechmeister, M., & Kürster, M. 2009, *A&A*, 496, 577, doi: [10.1051/0004-6361:200811296](https://doi.org/10.1051/0004-6361:200811296)